Inhibiting actin depolymerization enhances osteoblast differentiation and bone formation in human stromal stem cells

Chen, Li; Shi, Kaikai ; Frary, Charles; Ditzel, Nicholas; Hu, Huimin; Qiu, Weimin; Kassem, Moustapha

Published in:
Stem Cell Research

DOI:
10.1016/j.scr.2015.06.009

Publication date:
2015

Document version
Final published version

Stem Cell Research 15 (2015) 281–289

Contents lists available at ScienceDirect

Stem Cell Research

journal homepage: www.elsevier.com/locate/scr

Inhibiting actin depolymerization enhances osteoblast differentiation and bone formation in human stromal stem cells☆

Li Chen [a,*], Kaikai Shi [a], Charles Edward Frary [a], Nicholas Ditzel [a], Huimin Hu [a,b], Weimin Qiu [a], Moustapha Kassem [a,c]

[a] Molecular Endocrinology Laboratory (KMEB), Odense University Hospital, University of South Denmark, DK-5000 Odense C, Denmark
[b] Department of Spine Surgery, Honghui Hospital, Xi'an JiaoTong University College of Medicine, 710054 Xi'an, China
[c] Danish Stem Cell Center (DanStem), Panum Institute, University of Copenhagen, Copenhagen, Denmark

ARTICLE INFO

Article history:
Received 29 January 2015
Received in revised form 15 June 2015
Accepted 22 June 2015
Available online 30 June 2015

Keywords:
Actin polymerizing and depolymerizing factors
Osteoblastic differentiation
Bone formation
Human stromal stem cells

ABSTRACT

Remodeling of the actin cytoskeleton through actin dynamics is involved in a number of biological processes, but its role in human stromal (skeletal) stem cells (hMSCs) differentiation is poorly understood. In the present study, we demonstrated that stabilizing actin filaments by inhibiting gene expression of the two main actin depolymerizing factors (ADFs): Cofilin 1 (CFL1) and Destrin (DSTN) in hMSCs, enhanced cell viability and differentiation into osteoblastic cells (OB) *in vitro*, as well as heterotopic bone formation *in vivo*. Similarly, treating hMSC with Phalloidin, which is known to stabilize polymerized actin filaments, increased hMSCs viability and OB differentiation. Conversely, Cytocholasin D, an inhibitor of actin polymerization, reduced cell viability and inhibited OB differentiation of hMSC. At a molecular level, preventing Cofilin phosphorylation through inhibition of LIM domain kinase 1 (LIMK1) decreased cell viability and impaired OB differentiation of hMSCs. Moreover, depolymerizing actin reduced FAK, p38 and JNK activation during OB differentiation of hMSCs, while polymerizing actin enhanced these signaling pathways. Our results demonstrate that the actin dynamic reassembly and Cofilin phosphorylation loop is involved in the control of hMSC proliferation and osteoblasts differentiation.

1. Introduction

Cytoskeleton is a cellular scaffolding contained within cytoplasm. It maintains the cell shape, provides mechanical strength, directs locomotion, regulates chromosome separation in mitosis and meiosis and intracellular transport of organelles in cells (Doherty and McMahon, 2008; Van Troys et al., 2008). Actin microfilaments are the major structure of the cytoskeleton. The actin protein exists within cells in either globular/monomer (G-actin) or filamentous (F-actin) forms and thus in highly dynamic transitions of depolymerization and polymerizationin. During depolymerization, polymerized actin (F-actin) is severed/depolymerized and turns to monomer actin (G-actin). G-actin can be recycled, transferred back into filament form by an ADP-to-ATP exchange. ATP-actin becomes available for assembly and polymerization to F-actin (Ono, 2007). The process of assembly and disassembly of actin filaments in cells is regulated by actin depolymerizing factors (ADFs) that in mammals include: Cofilin1 (CFL1, non-muscle Cofilin), Cofilin2 (CFL2, muscle Cofilin), and Destrin (DSTN, also called ADF or Corn1). CFL1 is ubiquitously expressed, while CFL2 is only expressed in muscles. DSTN also exhibits ubiquitous expression, and its levels are about 5% to 10% of CFL1 levels (Vartiainen et al., 2002). Cofilin binds to actin monomers and filaments, causing depolymerization of actin filaments preventing their reassembly (Ghosh et al., 2004). Phosphorylation and dephosphorylation regulate Cofilin's binding and associating activity with actin (Lappalainen and Drubin, 1997; Maekawa et al., 1999). DSTN is a component protein in microfilaments. It severs actin filaments (F-actin) and binds to G-actin, thereby, sequestering actin monomers and preventing polymerization (Hawkins et al., 1993).

During lineage specific differentiation, human stromal (skeletal) stem cells (hMSCs) exhibit significant changes in morphology and actin cytoskeletal organization (McBeath et al., 2004; Yourek et al., 2007; Treiser et al., 2010). For example, during adipocyte differentiation, the cells undergo a morphological change from fibroblastic to spherical cells filled with lipid droplets (Fan et al., 1983). The change in cell shape takes place early in the differentiation process prior to the up-regulation of many adipocyte specific genes and in association with cytoskeletal changes including decreased actin synthesis and actin reorganization (Antras et al., 1989). Altered actin organization influences cytoskeletal tension which has been demonstrated to play a

☆ **Author contributions in the study**: L. Chen and M. Kassem designed the study, analyzed the data and wrote the manuscript; L. Chen performed most of the experiments with the help of K. Shi, C. E. Frary, N. Ditzel, H. Hu and W. Qiu. L. Chen directed the study.

* Corresponding author at: Odense University Hospital, Winslowsparken 25, 1th floor, DK-5000 Odense C, Denmark.
E-mail address: lchen@health.sdu.dk (L. Chen).

http://dx.doi.org/10.1016/j.scr.2015.06.009

role in adipogenesis in cultured MSCs (McBeath et al., 2004). Similarly, during chondrocyte differentiation of hMSCs, significant changes in cell shape that transform from a fibroblast-like to a circular morphology leading to a significant increase in cell volume (Xu et al., 2008). Similarly, the regulatory role of actin dynamics in chondrocyte differentiation has been supported by a number of experiments. Actin-disrupting compounds, such as cytochalasin D, stimulate chondrogenesis (Loty et al., 1995). In addition, intracellular kinases induced by adhesion signaling from extracellular matrix (ECM) proteins, regulate chondrocyte differentiation through changes in actin cytoskeleton (Woods et al., 2005, 2007; Nurminsky et al., 2007).

We became interested in the potential role of ADF genes and actin dynamics during osteoblast (OB) differentiation of hMSCs for several reasons. First, actin and microtubules are abundant in osteoblasts (Aubin et al., 1983; Arena et al., 1991). During OB differentiation, cell morphology is found to alter from fibroblast-like to cuboidal morphology; this is accompanied by changes in actin cytoskeleton (Lomri et al., 1987). Second, bone is a tissue that is sensitive to mechanical stimulation. The responses of osteoblastic cells to the applied mechanical forces are transmitted through plasma membrane adhesion molecules and induce alterations in actin cytoskeletal organization (Sakai et al., 2011). Third, some studies have reported that the upstream regulator of ADFs, such as Rho GTPase/Rho-Associated kinase (Rock), extracellular matrix (ECM) components, and adhesion kinases, act as regulators for OB differentiation (Harmey et al., 2004; Hamidouche et al., 2009; Mathews et al., 2012). However, evidence for the direct role of ADFs and dynamic organization of actin in MSCs biology and OB differentiation are not clear (Kawano et al., 2013; Shuang et al., 2013).

Thus, we examined the regulatory role of ADFs and actin cytoskeletal changes on lineage specific differentiation of hMSCs. We demonstrated that G-actin (monomer) and F-actin (polymerized) ratio was altered after induction of OB differentiation of hMSCs and was associated with significant changes in expression of ADFs. Lowering the expression levels of ADFs enhanced the polymerization of actin filaments, enhanced cell viability, and OB differentiation of hMSCs.

2. Materials and methods

2.1. Cell culture and OB differentiation of hMSCs

Primary hMSCs were isolated from human bone marrow aspirate as described previously (Stenderup et al., 2004). As a model for primary hMSCs, we employed the hMSC-TERT cell created in our laboratory by overexpression of human telomerase reverse transcriptase (hTERT) gene (Simonsen et al., 2002). hMSC-TERT exhibits all the characteristics of primary MSC *in vitro* and form normal heterotopic bone when implanted *in vivo* (Simonsen et al., 2002). Cells were grown in Minimal Essential Media (MEM) without Phenol red and L-glutamine, supplemented with 10% (v/v) fetal bovine serum (FBS), 2 mM Glutamax, 100 units/ml penicillin, and 100 μg/ml streptomycin (Gibco-Invitrogen, Carlsbad, CA), referred to as standard growth medium. *In vitro* OB differentiation of hMSC was carried out using OB induction medium containing standard growth medium supplemented with 10^{-8} M dexamethasone, 0.2 mM L-ascorbic acid, 10 mM β-glycerophosphate (Sigma), and 10 mM 1.25-vitamin-D3 (Leo® pharma).

2.2. Alkaline phosphatase (ALP) and Alizarin red S (AZR) staining

ALP cytochemical staining was performed on cultured cells by rinsing the cell layer with PBS followed by fixation in acetone/citrate (1.5:1, v:v) buffer (pH 4.2) for 5 minutes at room temperature. The cells were incubated with buffer containing 0.2 mg/ml naphthol AS-TR phosphate (Sigma). After incubation for one hour at 37 °C, the cell layer was washed with deionized water. Alizarin red S staining was employed to assess the presence of in vitro formed mineralized matrix. The medium was removed, and the cell layer was rinsed with PBS and fixed in 70% ethanol for 1 hour at -20 °C. The cell layer was washed with deionized water. The fixed cells were stained with 40 mM Alizarin red S pH 4.2 (Sigma) for 10 minutes at room temperature. The cell layer was washed with deionized water. For quantitative assessment of the degree of mineralization, the color was eluted by 10% (wt/vol) cetylpyridinium chloride (Sigma) for 1 h and quantified by spectrophotometric absorbance measurements at OD570nm (Gregory et al., 2004).

2.3. ALP activity assay

ALP activity assay was performed in the96-well plate. Cell number (i.e. the number of viable cells) was determined by adding the CellTiter-Blue solution (Promega) for 1 hour and measured the fluorescence at wavelength of $579_{Ex}/584_{Em}$. The cells were then rinsed with PBS and fixed in 3.7% formaldehyde-90% ethanol for 30 seconds at room temperature. A reaction mixture containing 100 μl 50 mM $NaHCO_3$, 1 mM $MgCl_2$ (Sigma) and 1 mg/ml of p-nitrophenyl phosphate (Sigma) was added into each well and incubated at 37 °C for 20 minutes. The reaction was stopped by adding 50 μl of 3 M NaOH. Absorbance was determined at 405 nm in an ELISA microplate reader. ALP enzymatic activity was normalized to cell number in each well.

2.4. Cell transfection

Small interfering RNA (siRNA) duplex oligos targeting DSTN, CFL1, CFL2, LIMK1, as well as non-targeting duplex oligo (siRNA negative controls) were purchased from Ambion (Life Technology Inc.). These reagents were transfected into hMSC-TERT at a final concentration of 12 nM for siRNA. All transfections were performed using Lipofectamine2000 Transfection Reagent (Invitrogen), according to the manufacturer's instructions.

2.5. Treatment with Cytochalasin D and Phalloidin during OB differentiation in hMSCs

hMSCs were seeded in 24-well plate or 96-well plate and induced to osteogenic differentiation as described above. The media was changed every third day. Before media change, the cells were pre-treated with Cytochalstin D (Sigma, C8273) (1-20 uM) for 1 h or Phalloidin (Sigma, P2141) (0-6 uM) for 3 h. After treatment, cells were washed and incubated in differentiation medium. Equal volumes of DMSO solution was added into the corresponding controls wells.

2.6. Actin staining and cell shape detection by high content cellomic analysis

Cells were seeded at a density of 2000 cells per well into clear bottom 96-well CellCarrier™ microtiter plates (PerkinElmer), the Operetta® High Content Imaging System was used to study the cellular changes. Cells were washed with PBS, fixed with 4% formaldehyde for 30 min, and permeabilized with 0.1% Triton™-X-100 for 10 min. Subsequently, the cells were stained with a dye solution containing 10 μg/mL 4',6-diamidino-2-phenylindole (DAPI) (Sigma-Aldrich®, D8417) and 5 μg/mL Phalloidin-TRITC (Sigma-Aldrich®, P1951). Images were acquired on an Operetta® high content image System (Perkin Elmer) using a 10X high NA (numerical apertures) objective in wide-field mode. All pictures were acquired with the same contrast and brightness parameters. For quantitative analyses, individual cells were segmented based on the DAPI nuclear stain using the Find Nuclei building block in the Harmony® High Content Imaging and Analysis Software. The following parameters were determined per cell: cell size (area) (μm2), cell length (μm), cell width (μm), cell roundness, cell ratio (width to length), nuclear size (μm2), and nuclear roundness. The staining intensity of TRITC was measured in each well and normalized to the cell number.

2.7. G-actin/F-actin assay

The filamentous (F-actin) and monomer actin (G-actin) in cells were quantitated by G-actin/F-actin in vivo assay kit as manufacturer's instructions (Cytoskeleton Inc.). Cells were harvested by scraping in lysis and F-actin stabilization buffer. The homogenates were incubated at 37 °C for 10 mins, transferred to a pre-warmed (37 °C), ultracentrifuge (SORVALL/Thermo Scientific), and spun at 100,000 g for 1 h at 37 °C to separate the globular (G)-actin (supernatant) and filamentous (F)-actin fractions (pellet). The pellets were re-suspended in ice-cold depolymeraizing buffer. All samples were diluted with the appropriate loading buffer and boiled for 5 min. The samples were further separated by sodium dodecyl sulfate polyacrylamide gel electrophoresis (SDS-PAGE) and Western blot analysis. The blots were scanned and the protein bands were subjected to intensity quantification in ImageJ® software. The ratios of F-actin or G-actin in cells were calculated according to the density.

2.8. Western blot analysis

hMSC cells were washed in PBS and lysed in RIPA buffer (Invitrogen) supplemented with protease inhibitors (Roche). After 1 h incubation at 4 °C, samples were centrifuged for 10 min at 12,000 rpm at 4 °C. Protein concentration was determined with Pierce Coomassie^{Plus} Bradford assay (Thermo Fisher Scientific), and equal amounts of protein were loaded on a 10% polyacrylamide gel (Invitrogen). Blotted nitrocellulose membranes were incubated with antibodies overnight at 4 °C. Membranes were incubated with HRP conjugated anti-mouse or anti-rabbit secondary antibody (Santa Cruz Biotechnology) for 45 min at room temperature. The protein bands were visualized with Amersham ECL chemiluminescence detection system (GE Healthcare Bio-Sciences Corp) in X-ray films. Results were scanned and edited in Photoshop®. Antibodies (total or phosphor) specific for AKT, SMAD1/5/8, ERK, RUNX2 and LIMK1 were obtained from Cell Signaling Technology®. Antibodies for phos-CFL1, total CFL1 were purchased from Abcam®. Antibodies for DSTN and α-tubulin were bought from Sigma®. The antibody for actin was bought with G-actin/F-actin in vivo assay kit (Cytoskeleton Inc.). All antibodies were used at 1:1000 dilutions except α-tubulin antibody (1:5000) in this study.

2.9. Quantitative real-time reverse transcription polymerase chain reaction (qRT-PCR)

For gene expression, total RNA was extracted with TriZoL reagent (Invitrogen), and cDNA was prepared using revert Aid H minus first strand cDNA synthesis kit (Fermentas). The primers that were employed are listed in Table S1. The PCR products were visualized in real-time using SYBR Green I Supermix (Bio-Rad) and an iCycle instrument (Bio-Rad) using standard curve protocols normalized to beta-2-microglobulin (B2m). The quantitative data presented are an average of duplicate or triplicate per independent experiment.

2.10. In vivo heterotopic bone formation assay

hMSC (5×10^5cells/sample) were loaded on 40 mg wet hydroxyapatite/tricalcium phosphate (HA/TCP) (Zimmer), incubated at 37 °C overnight, and implanted subcutaneously on the dorsal side of 8-week-old NOD.CB17-Prkdcscid/J mice (NOD/SCID) as previously described (Stenderup et al., 2004; Abdallah et al., 2008). Implants were removed after 8 weeks, fixed in 4% paraformaldehyde, decalcified in formic acid, and embedded in paraffin. Sections (4-μm) were cut and stained with eosin/hematoxlyin (Bie&Berntsens, Denmark). Bone volume per total volume was quantified as previously described (Abdallah et al., 2008). All animal experiments were carried out in accordance with permissions issued by The Animal Experiments Inspectorate.

2.11. Statistical analysis

Data are presented as mean ± standard error of the mean (SEM). Statistical testing was performed using Student's t-test to detect differences between groups. Differences were considered statistically significant at $P < 0.05$ (*), $P < 0.001$ (**).

3. Results

3.1. Changes in cytoskeletal proteins expression during osteoblast (OB) differentiation of hMSCs

We observed an association of changes in actin forms and expressions of ADFs during in vitro OB differentiation of hMSCs. In undifferentiated hMSCs, we measured that 46% of actin is soluble (G-actin) and 54% is polymeric (F-actin). During the initial differentiation, until day 3, there was a decrease of F-actin (to around 40%) and increase of G-actin (up to around 60%). Following OB differentiation induction, we observed a gradual increase in polymeric actin (F-actin) that reached maximal levels on day 13 (F-actin, 63%) (Fig. 1A). The change in actin forms during OB differentiation was associated with changes in the expression levels of key ADFs. Levels of total CFL1 remained stable throughout the differentiation process, but levels of phosphorylated (P-) CFL1 (inactive form) were increased. Conversely, DSTN levels increased at the beginning of differentiation and decreased following induction of OB differentiation. The LIMK1 phosphorylation increased during OB differentiation, while the total LIMK1 was unchanged (Fig. 1B).

3.2. siRNA-mediated knock-down of Cofilin and Destrin expression enhanced OB differentiation of hMSCs in vitro and heterotopic bone formation in vivo

In order to detect the role of ADFs and actin dynamics in OB differentiation, we employed siRNA-mediated knock down of the two key ADFs and examined the effects on OB differentiation of hMSCs. Knock down of CFL1 or DSTN in hMSCs blocked the protein expression in cells (around 95%, see Fig. S1 for real time PCR and Western blot analysis). Knocking down of CFL1 and DSTN both increased viable cell numbers on day 7 of OB differentiation, and decreasing DSTN has significant

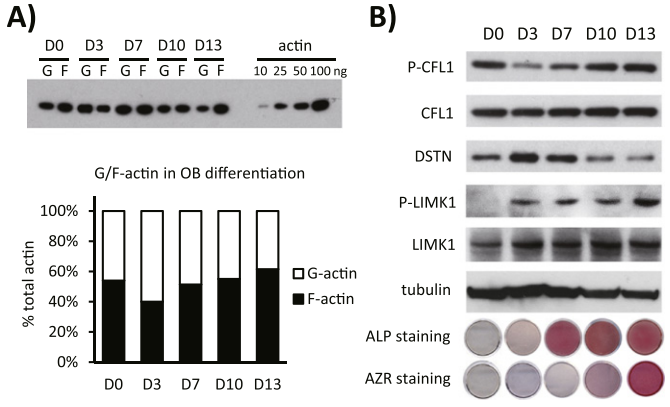

Fig. 1. Changes in monomeric (G-actin), polymeric actin (F-actin) and actin depolymerizing factors (ADFs) during OB differentiation in hMSCs. Human stromal (skeletal) stem cells (hMSCs) were induced to osteoblast (OB) differentiation as evidenced by positive cytochemical staining of alkaline phosphatase (ALP) and Alizarin red (AZR) presented as scanned pictures of culture dishes (B). Protein samples were harvested at differentiation day 0, 3, 7, 10 and 13. A) Actins were separated by ultracentrifugation to F-actin and G-actin and subjected to Western Blot analysis (upper part) for quantitation of the ratio of F-actin and G-actin in cells (lower part). D: Days after differentiation induction. B) Total cell lysates were subjected to Western blot analysis of ADFs and LIMK1. Alpha-tubulin was measured as protein loading control. Results show the representational data derived from at least three independent experiments.

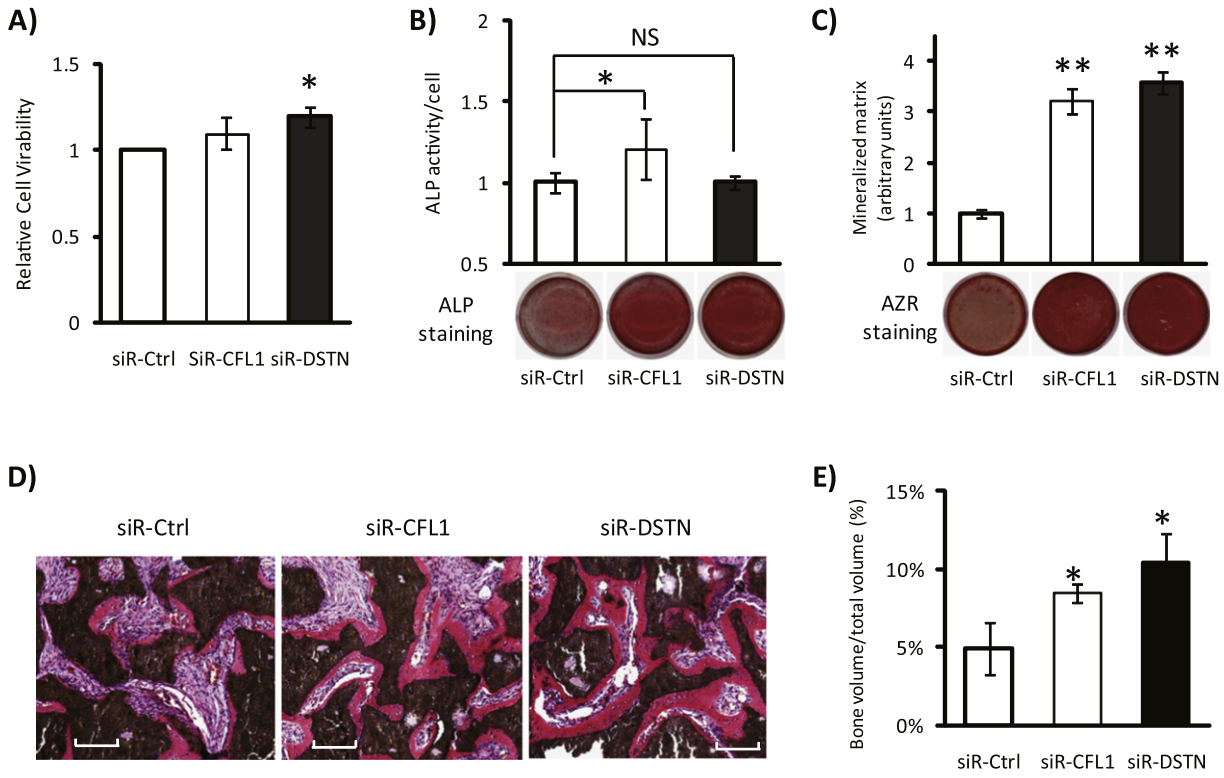

Fig. 2. siRNA-mediated knockdown of CFL1 and DSTN enhanced osteoblast differentiation in vitro and heterotopic bone formation of hMSCs in vivo. Human stromal (skeletal) stem cells (hMSCs) were cultured and transfected with siRNAs for CFL1, DSTN or with non-target siRNA (control). In vitro osteoblast (OB) differentiation: Twenty four hours following transfection, the cells were induced to OB differentiation as described in Material & Methods. Cell viability (A), alkaline phosphatase (ALP) activity and ALP staining (B) and mineralized matrix formation visualized by Alizarin red S (AZR) staining and quantitation (C) were performed. Results were presented as the mean ± standard error of the mean (SEM) of at least three independent experiments. For in vivo heterotopic bone formation, siRNA-transfected cells were implanted coupled to hydroxyapatite/tricalcium phosphate (HA/TCP) scaffold subcutaneously into immune deficient NOD/SCID mice. (D) H&E staining was performed after 8 weeks of implantation to quantitate newly formed bone. Bone tissue (red); HA/TCP scaffold (brown). Scale bar: 250 μm. (E) Bone formation was quantitated using image analysis and expressed as bone area divided by total area (n = 7 implants per treatment). *P < 0.05; **P < 0.001.

effect (Fig. 2A & Fig. S2C). siRNA-mediated knockdown of CFL1 enhanced OB differentiation of hMSCs evidenced by significant increase in ALP staining at day 7 (Fig. 2B) and mineralized matrix formation at day 10 (Fig. 2C) of OB differentiation. For DSTN, the effects of knock down were more pronounced on mineralized matrix formation (Fig. 2C). Similar results were observed upon siRNA-mediated knock down of CFL1 and DSTN in human bone marrow derived primary MSC (Fig. S2). Interestingly, knocking down of CFL2, a muscle specific ADF, did not lead to detectable effects on OB differentiation (Fig. S3).

To investigate the function of ADFs on bone formation, hMSCs transfected with siRNA against CFL1 and DSTN or corresponding non-target controls, were implanted subcutaneously into immune deficient mice. Heterotopic bone formation was significantly increased (more than 1.5 times) in implants of hMSCs deficient in CFL1 or DSTN compared with control (Fig. 2D, E).

3.3. siRNA-mediated knockdown of CFL1 and DSTN increased polymerized actin (F-actin) and not change cell morphology of hMSCs

To further detect the effects of siRNA-mediated knock down of CFL1 and DSTN on actin dynamics, we stained cells by TRITC-coupled Phalloidin that binds polymerized actin filaments (F-actin). We examined the morphological changes in the cells using high content imaging (Fig. 3A). >Knockdown of CFL1 or DSTN did not affect cellular morphology i.e. nuclear size, nuclear roundness, cell size, cell width, cell length, ratio of cell width to length, and cell roundness (Fig. 3B). We detected a significant increase in the intensity of TRITC-Phalloidin staining (Fig. 3C) suggesting increased polymerized actin filament formation. This was confirmed by direct measurement of F actin/G actin ratio (Fig. 3D).

3.4. Cytochalasin D and Phalloidin treatment led to significant changes in OB differentiation in hMSCs.

siRNA-mediated knock down of CFL1 or DSTN in hMSCs increased polymerized F-actin that was associated with enhanced OB differentiation of hMSCs. To confirm that increased levels of actin polymerization exert significant increase on the proliferation and OB differentiation of hMSCs, we treated hMSCs with Cytochalsin D and Phalloidin. Cytochalasin D promotes depolymerizing actin and phalloidin stabilizes actin filaments (Fig. S4). Treating hMSCs with Cytochalasin D inhibited OB differentiation evidenced by a dose-dependent decrease in ALP activity and decreased mineralized matrix formation (Fig. 4A). Conversely, Phalloidin treated hMSCs exhibited increased ALP activity and mineralized matrix formation (Fig. 4B). The effects of Cytochalasin D and Phalloidin on OB differentiation were also confirmed in human primary bone marrow MSCs (Fig. S5) and mouse bone marrow MSCs (Fig. S6).

3.5. Inhibition of LIMK1 inhibited phosphorylation of Cofilin and OB differentiation of hMSCs.

During the course of OB differentiation of hMSCs, phosphorylation of Cofilin was up-regulated (Fig. 1) suggesting that phosphorylation of Cofilin mediates changes in OB differentiation. Cofilin is inactivated by the phosphorylation at Ser3 by LIM kinase (LIMK) and activated by phosphatase SSH1. The spatially coordinated activities of LIMK and Cofilin phosphatase are required for regulating actin dynamics and controlling actin-dependent cellular processes (Yang et al., 1998). To examine whether the Cofilin phosphorylation loop plays a regulatory role in

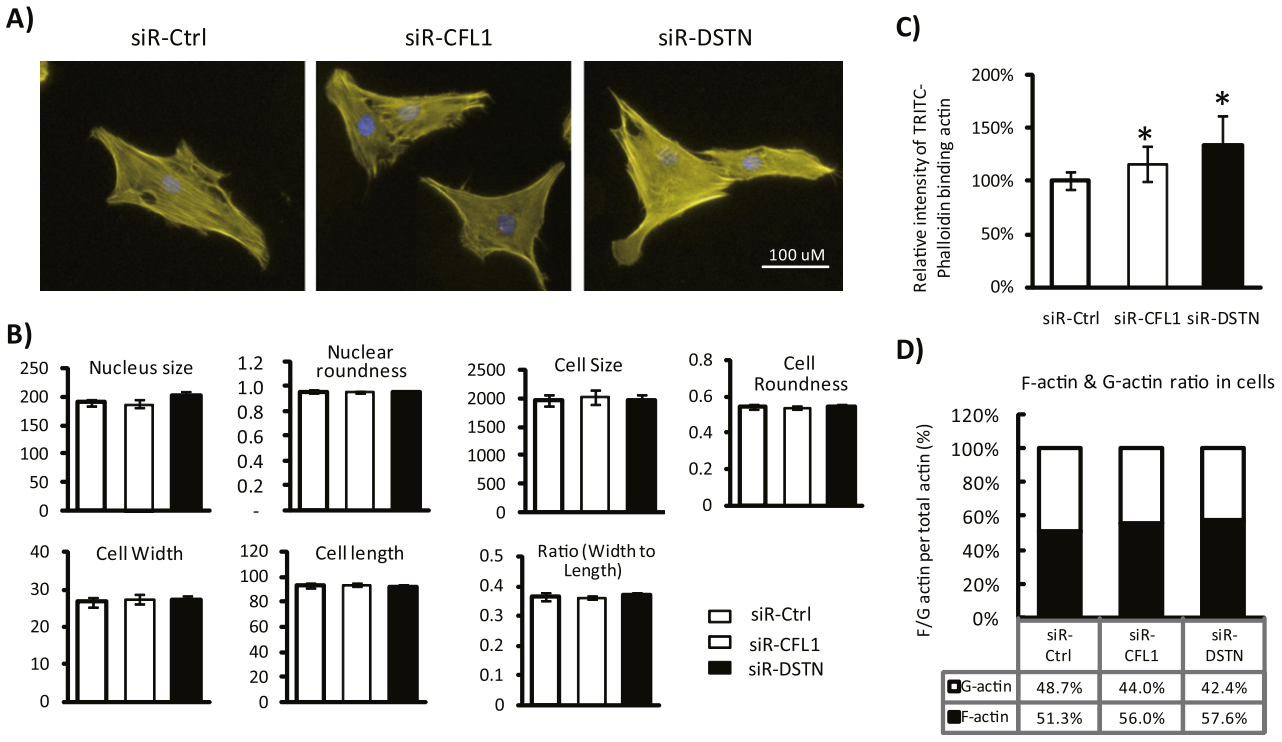

Fig. 3. siRNA-mediated knockdown of CFL1 and DSTN increased polymerized actin (F-actin) levels but did not change cell morphology of human stromal (skeletal) stem cells (hMSCs). hMSCs were cultured and transfected with siRNAs for CFL1, DSTN or with non-target siRNA (control). After 24 hours, the cells were stained with TRITC-Phalloidin and DAPI (A). Scale bar: 100 μm. Analysis of changes of cell morphology was carried out by the Operetta® High Content Imaging System. Cell morphology and intensity of TRITC-Phalloidin binding actin were analyzed by the Harmony® software (B & C). At the same time, transfected cells were harvested, cellular actin was separated by ultracentrifugation into F-actin and G-actin by F-actin/G-actin in vivo assay kit. Quantitation of the ratio of F-actin and G-actin per total actin (%) was determined (D). Results are derived from at least three independent experiments.

OB differentiation of hMSCs, we treated hMSC with LIMK inhibitor (LIMKi). LIMK inhibitor reduced the phosphorylated Cofilin in a dose dependent manner from 100 nM to 10 μM (Fig. 5A), and concomitantly inhibited OB differentiation, as revealed by a dose-dependent decrease in cell viability, ALP staining and activity, as well as a reduction in mineralized matrix formation shown by Alizarin red (AZR) staining

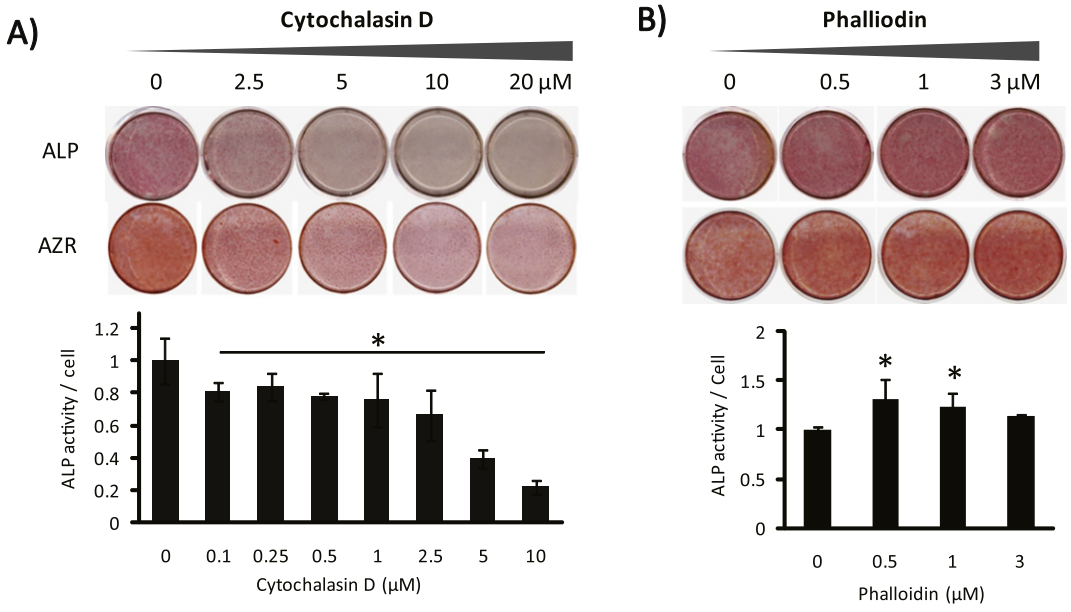

Fig. 4. Cytochalsin D and Phalloidin treatment induced significant changes in osteoblast OB differentiation of human stromal (skeletal) stem cells (hMSCs). hMSCs were induced to OB differentiation, and the cells were treated with Cytochalasin D (1 hour, every other day) and Phalloidin (3 hours, every other day) at the indicated concentrations. Alkaline phosphtase (ALP) staining was performed at OB differentiation Day 7. Alizarin red (AZR) staining was performed at OB differentiation Day 12. Data represents results from three independent experiments. *P < 0.05, **P < 0.001.

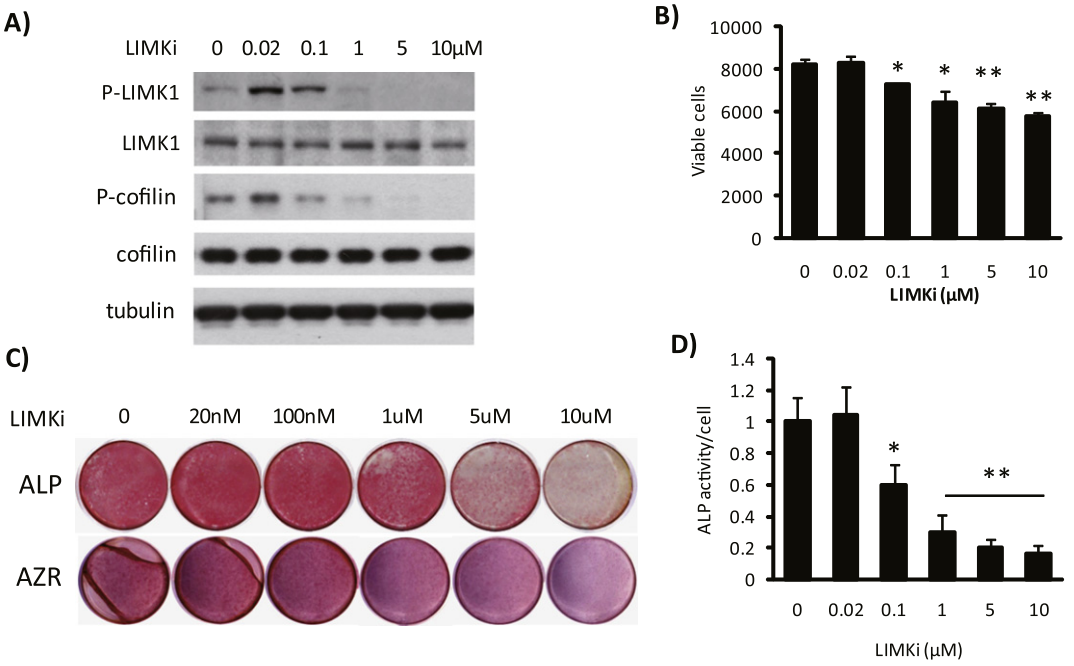

Fig. 5. Inhibition of LIMK reduced phosphorylation of Cofilin and inhibited osteoblast (OB) differentiation of hMSCs. Human bone marrow stromal (skeletal) stem cells (hMSCs) were cultured and induced to OB differentiation. The cells were treated with a LIMK inhibitor (LIMKi) at the indicated concentrations for 14 days. (A) The phosphorylated Cofilin, total Cofilin, and alpha-tubulin were measured by Western blot on OB differentiation Day 9. (B) Cell viability and alkaline phosphatase (ALP) activity were determined at OB differentiation Day 7. (C) Staining for alkaline phosphatase was performed at OB differentiation Day 7 and for mineralized matrix formation by Alizarin red (AZR) were performed at OB differentiation Day 14. *P < 0.05, **P < 0.001. Data represents representational results from at least three independent experiments.

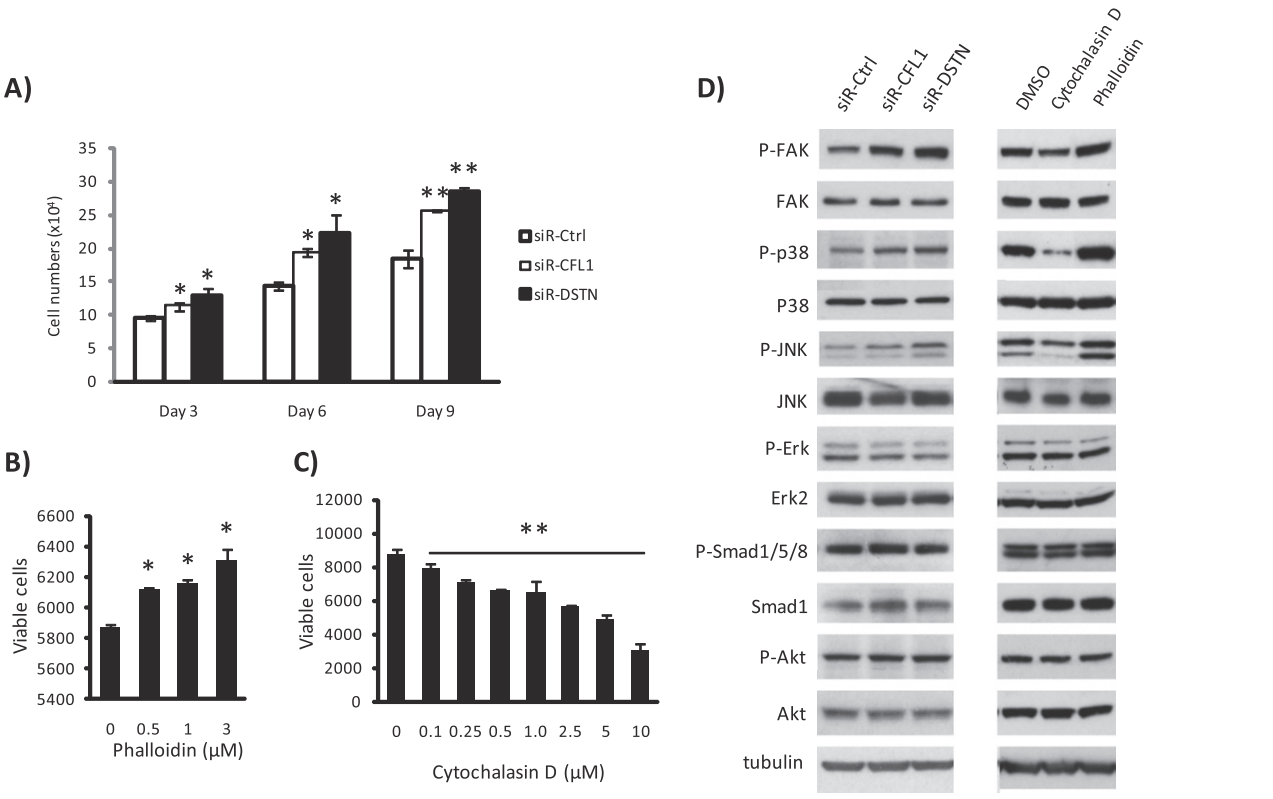

Fig. 6. Changes in actin polymerization led to alterations in cell viability and multiple intracellular signaling pathways. Human stromal (skeletal) stem cells (hMSCs) were cultured and transfected with siRNAs for CFL1, DSTN, with non-target siRNA (control) (A), or treated with Phalloidin or Cytochalasin D in the indicated concentrations (B, C). Same amount cells were seeding and induced to osteoblast (OB) differentiation as described in Material & Methods. (A) Cell numbers were determined during the OB differentiation on Day (D) 3, 6, and 9. (B, C) Cell viability was measured on day 7 in hMSCs treated with Phalloidin (3 hours each other day) or Cytochalsin D (1 hour each other day) during OB differentiation. (D) The activation of intracellular signaling pathways (FAK, P38, JNK, Erk, Akt, Smad1/5/8) was analyzed by Western Blot analysis. Left part: hMSCs were transfected by siRNA for non-target control, or CFL1 and DSTN. Right part: hMSCs were treated by Cytochalasin D (5 μM, 1 hour) or Phallodin (3 mM, 3 hours). Total cell lysates were subjected Western blot analysis. Data represents representative result from at least three independent experiments.

(Fig. 5B, C). siRNA-mediated knock down of LIMK1 in hMSCs led to similar results (Fig. S7). We also checked the knockdown of phosphatase SSH1 in hMSCs, but the knockdown of SSH1 in cells induced severe cell death of hMSCs (data not shown).

3.6. Changes in actin dynamics affect cell viability

As mentioned above, change in actin dynamic assembly was associated with changes in cell viability. To further analyze this phenomenon, we determined changes in the viable cells during the course of OB differentiation. siRNA-mediated knock down of CFL1 or DSTN in hMSCs increased the cell proliferation (Fig. 6A) suggesting that enhancing actin polymerization improves cell survival. This notion was corroborated by treating the cells with Cytochalasin D and Phalloidin. Cytochalasin D reduced and Phalloidin increased the number of viable cells (Fig. 6B, C). Similarly, LIMKi reduced viable cell numbers (Fig. 5B).

3.7. Changes in actin dynamics are associated with alterations in FAK, p38, and JNK signalling

Since changes in actin dynamics affects hMSCs viability and differentiation, we examined changes in a number of signaling pathways known to be important in hMSCs biology. We detected increased activation of focal adhesion kinase (FAK), p38, and JNK kinases following siRNA-mediated inhibition of CFL1 and DSTN expression and following treatment with Phalloidin. The opposite effects were observed following treatment with Cytochalasin D. We did not detect changes in the activation at ERK, Akt, and Smad1/5/8 pathways (Fig. 6D)

4. Discussion

Actin cytoskeleton undergoes cycles of actin assembly that exists in two states: a monomeric state (globular, G-actin) and a fibrous state (filamentous, F-actin). A variety of actin filament lengths and shapes are established by actin-depolymerizing factors (ADFs) and other actin binding factors that are responsible for changes in structure and morphology of eukaryotic cells under different physiological conditions. Among the ADFs, active Cofilin (non-phosphorylated) and DSTN bind to F-actin without capping and severe the actin filament (F-actin) into monomers free ends actin (G-actin). Polymerization of actin is regulated by a series of kinases, such as GTPase RhoA, RhoA kinase (ROCK), and LIM kinases, which phosphorylates the actin depolymerizing protein Cofilin and stabilizes actin filaments (Lodish et al., 2000). In the present study, we demonstrated that changes in the levels of ADFs lead to changes in viability and OB differentiation of hMSCs. siRNA-mediated knocking down of CFL1 or DSTN enhanced OB differentiation and heterotopic bone formation of hMSCs *in vivo*. Our results confirm part of the findings in previous related studies (Rodriguez et al., 2004; Sonowal et al., 2013), and fulfil the map where the balance of actin assembly (depolymerization and polymerization) is a regulatory factor for viability and OB differentiation of hMSCs and that these effects are mediated through a number of intracellular signaling pathways (Fig. 7).

We observed that changes in actin dynamics induce alterations in cell viability. A number of studies have indicated that factors regulating actin cytoskeleton, can exert regulatory functions on cell proliferation. For example, Cofilin phosphorylation mediates proliferation in response to platelet-derived growth factor (PDGF) in rat aortic smooth muscle cells (Won et al., 2008), and inhibition of Cofilin-1 expression blocks PDGF-induced proliferation in endometrium (Wang et al., 2013). Conversely, ectopic-expression of of ADFs and Cofilin suppress the motility and proliferation of human lung cancer cells (Lee et al., 2005). These results suggest that direct regulation of ADFs and actin reassembly can affect cell proliferation and viability. It is possible that ADFs and actin assembly can exert direct regulation of cell cycle genes. It is also possible that actin reassembly provide mechanical structure for cell division (Warn and Magrath, 1983; Kaji et al., 2003) and the mitotic process (Tsai et al., 2009).

ADFs have been reported to regulate cell differentiation in a number of tissues. CFL1 and DSTN are required for ureteric bud branching morphogenesis (Kuure et al., 2010). Conditional deletion of CFL1 in neuronal cells enhances cell differentiation (Bellenchi et al., 2007). In addition, Cofilin and phospho-Cofilin expression are increased in conditions favoring myofibroblast differentiation. Knockdown of CFL1 inhibited collagen gel contraction and reduced myofibroblast differentiation (Pho et al., 2008). Moreover, CFL1 has been reported to be activated at the time of podosome belt assembly during osteoclast differentiation (Blangy et al., 2012). We report that ADFs participate in the regulation of OB differentiation of hMSCs and provide a link between changes in cytoskeleton and lineage specification of hMSCs.

Human DSTN and CFL1 are more than 70% identical in amino acid sequence. DSTN has a much higher actin depolymerizing activity than Cofilin (Yeoh et al., 2002) which is explained by sequence differences at the F-actin-binding site (Pope et al., 2004). CFL1 deficiency is embryonic lethal at E11.5–12.5 and displays defects in neural tube closure and neural crest cell migration despite high expression of DSTN (Gurniak et al., 2005). DSTN deficient mice are viable but have corneal defects leading to eventual blindness in adult mice. Conversely, DSTN deficient mice have normal brain development (Ikeda et al., 2003). We found that lowering both DSTN and CFL1 could enhance OB differentiation. However, part of DSTN's effect on cell differentiation may be mediated through enhancement of cell viability. The observed differences can be caused by differences in binding affinity with actin or actin depolymerization efficiency. Further studies are needed to study these hypotheses.

In eukaryotic cells, Cofilin is an important dynamic regulator of actin assembly. Its activity is regulated by phosphorylation at the N-terminal

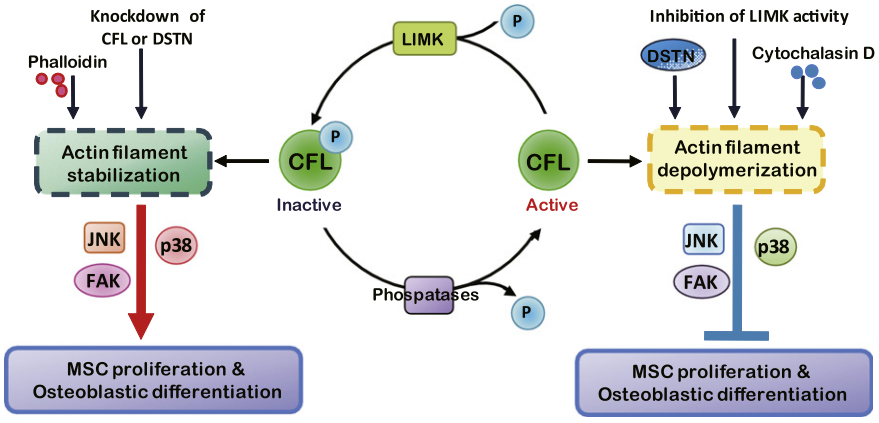

Fig. 7. A working model illustrating the effect of changes in actin depolymerizing factors (ADFs) on cell viability and osteoblast differentiation of human stromal (skeletal) stem cells (hMSCs). CFL: Cofilin; DSTN: Destrin; LIMK: LIM kinase; FAK: Focal adhesion kinase; p38: p38 mitogen-activated protein kinase; JNK: c-Jun N-terminal kinase.

Serine 3 that inhibits its activity and the binding to G-actin. Dephosphorylation at Ser-3 recovers CFL1 activity. LIM kinase (LIMK) is one of the key kinases that regulate the activity of ADFs through phosphorylation of the actin depolymerizing protein Cofilin (inactive Cofilin) thereby stabilizing actin filament formation within the cell. In our study, inhibition of LIMK by a chemical inhibitor or specific siRNA, resulted in inhibition of activation and phosphorylation of Cofilin and inhibition of hMSCs viability and OB differentiation. Our findings provide a molecular explanation to previous observations of presence of low bone mass phenotype in LIMK 1 deficient mice (Kawano et al., 2013). In addition to LIMK1, other upstream kinases are involved in the regulation of Cofilin phosphorylation and its activity. The Rho small GTPase family and its downstream effectors, Rho-associated kinase (ROCK) and p21-activated kinase (PAK), can both phosphorylate activate LIMK and therefore inactivate Cofilin (Zigmond, 1996; Bernard, 2007). Another kinase named testis-specific kinase (TESK) can inactivate Cofilin through phosphorylation and is dependent on signaling through integrin (Toshima et al., 2001). In contrast, slingshot (SSH) phosphatase and chronophin (CIN) have been shown to activate Cofilin by dephosphorylating at Serine 3 residue and suppressing the assembly of actin filaments (Niwa et al., 2002; Huang et al., 2006). Many studies have demonstrated that the above mentioned kinases, such as Rho, Rac, Rock, LIMK and 14-3-3, are possible regulators of OB differentiation (Liu et al., 2007; Yamashita et al., 2008; Prowse et al., 2013). Our study suggest that these signaling pathways can mediate their biological effects through changes in actin cytoskeletal organization through conversion of ADFs and Cofilin in cells and further signaling through FAK, JNK, and p38 MAP kinases signaling pathways. Several studies have reported that the main actin binding proteins in vertebrate such as thymosin-beta 4 and profilin regulate cell differentiation, e.g. odontogenic differentiation or sternum development (Lee et al., 2013; Someya et al., 2015) related to Akt, P38, JNK, ERK, BMP pathways, followed by transcriptional regulation of Runx2 and Osterix (Lee et al., 2013; Sonowal et al., 2013; Someya et al., 2015). Since there exists over 60 families of actin-binding proteins that influence actin filament assembly/disassembly, it will be very interesting to explore the networks associated with actin assembly (composed by kinases and actin binding proteins) during different lineage commitment and differentiations of stem cells.

Acknowledgments

We are grateful to Tina Kamilla Nielsen and Lone Christiansen for their technical assistance. This study is supported by a grant from the Novo Nordisk Foundation (L.C) and ECTS Postdoctoral Fellowship 2012 (L.C.). All authors have no conflicts of interest.

Appendix A. Supplementary data

Supplementary data to this article can be found online at http://dx.doi.org/10.1016/j.scr.2015.06.009.

References

Abdallah, B.M., Ditzel, N., Kassem, M., 2008. Assessment of bone formation capacity using in vivo transplantation assays: procedure and tissue analysis. Methods Mol. Biol. 455, 89–100. http://dx.doi.org/10.1007/978-1-59745-104-8_6.

Antras, J., Hilliou, F., Redziniak, G., Pairault, J., 1989. Decreased biosynthesis of actin and cellular fibronectin during adipose conversion of 3 T3-F442A cells. Reorganization of the cytoarchitecture and extracellular matrix fibronectin. Biol. Cell. 66, 247–254.

Arena, N., Venti, G., Becchetti, E., Baroni, T., Donti, E., Paludetti, G., Bodo, M., 1991. Characterization of the cytoskeleton in human normal and otosclerotic osteoblast-like cells. Acta Anat. (Basel) 141, 311–315.

Aubin, J.E., Alders, E., Heersche, J.N., 1983. A primary role for microfilaments, but not microtubules, in hormone-induced cytoplasmic retraction. Exp. Cell Res. 143, 439–450.

Bellenchi, G.C., Gurniak, C.B., Perlas, E., Middei, S., Ammassari-Teule, M., Witke, W., 2007. N-cofilin is associated with neuronal migration disorders and cell cycle control in the cerebral cortex. Genes Dev. 21, 2347–2357. http://dx.doi.org/10.1101/gad.434307.

Bernard, O., 2007. Lim kinases, regulators of actin dynamics. Int. J. Biochem. Cell Biol. 39, 1071–1076. http://dx.doi.org/10.1016/j.biocel.2006.11.011.

Blangy, A., Touaitahuata, H., Cres, G., Pawlak, G., 2012. Cofilin activation during podosome belt formation in osteoclasts. PLoS One 7, e45909. http://dx.doi.org/10.1371/journal.pone.0045909.

Doherty, G.J., McMahon, H.T., 2008. Mediation, modulation, and consequences of membrane-cytoskeleton interactions. Annu. Rev. Biophys. 37, 65–95. http://dx.doi.org/10.1146/annurev.biophys.37.032807.125912.

Fan, J.Y., Carpentier, J.L., van Obberghen, E., Grunfeld, C., Gorden, P., Orci, L., 1983. Morphological changes of the 3 T3-L1 fibroblast plasma membrane upon differentiation to the adipocyte form. J. Cell Sci. 61, 219–230.

Ghosh, M., Song, X., Mouneimne, G., Sidani, M., Lawrence, D.S., Condeelis, J.S., 2004. Cofilin promotes actin polymerization and defines the direction of cell motility. Science 304, 743–746. http://dx.doi.org/10.1126/science.1094561.

Gregory, C.A., Gunn, W.G., Peister, A., Prockop, D.J., 2004. An Alizarin red-based assay of mineralization by adherent cells in culture: comparison with cetylpyridinium chloride extraction. Anal. Biochem. 329, 77–84. http://dx.doi.org/10.1016/j.ab.2004.02.002.

Gurniak, C.B., Perlas, E., Witke, W., 2005. The actin depolymerizing factor n-cofilin is essential for neural tube morphogenesis and neural crest cell migration. Dev. Biol. 278, 231–241. http://dx.doi.org/10.1016/j.ydbio.2004.11.010.

Hamidouche, Z., Fromigue, O., Ringe, J., Haupl, T., Vaudin, P., Pages, J.C., Srouji, S., Livne, E., Marie, P.J., 2009. Priming integrin alpha5 promotes human mesenchymal stromal cell osteoblast differentiation and osteogenesis. Proc. Natl. Acad. Sci. U. S. A. 106, 18587–18591. http://dx.doi.org/10.1073/pnas.0812334106.

Harmey, D., Stenbeck, G., Nobes, C.D., Lax, A.J., Grigoriadis, A.E., 2004. Regulation of osteoblast differentiation by Pasteurella multocida toxin (PMT): a role for Rho GTPase in bone formation. J. Bone Miner. Res. 19, 661–670. http://dx.doi.org/10.1359/JBMR.040105.

Hawkins, M., Pope, B., Maciver, S.K., Weeds, A.G., 1993. Human actin depolymerizing factor mediates a pH-sensitive destruction of actin filaments. Biochemistry 32, 9985–9993.

Huang, T.Y., DerMardirossian, C., Bokoch, G.M., 2006. Cofilin phosphatases and regulation of actin dynamics. Curr. Opin. Cell Biol. 18, 26–31. http://dx.doi.org/10.1016/j.ceb.2005.11.005.

Ikeda, S., Cunningham, L.A., Boggess, D., Hawes, N., Hobson, C.D., Sundberg, J.P., Naggert, J.K., Smith, R.S., Nishina, P.M., 2003. Aberrant actin cytoskeleton leads to accelerated proliferation of corneal epithelial cells in mice deficient for destrin (actin depolymerizing factor). Hum. Mol. Genet. 12, 1029–1037.

Kaji, N., Ohashi, K., Shuin, M., Niwa, R., Uemura, T., Mizuno, K., 2003. Cell cycle-associated changes in Slingshot phosphatase activity and roles in cytokinesis in animal cells. J. Biol. Chem. 278, 33450–33455. http://dx.doi.org/10.1074/jbc.M305802200.

Kawano, T., Zhu, M., Troiano, N., Horowitz, M., Bian, J., Gundberg, C., Kolodziejczak, K., Insogna, K., 2013. LIM kinase 1 deficient mice have reduced bone mass. Bone 52, 70–82. http://dx.doi.org/10.1016/j.bone.2012.09.024.

Kuure, S., Cebrian, C., Machingo, Q., Lu, B.C., Chi, X., Hyink, D., D'Agati, V., Gurniak, C., Witke, W., Costantini, F., 2010. Actin depolymerizing factors cofilin1 and destrin are required for ureteric bud branching morphogenesis. PLoS Genet. 6, e1001176. http://dx.doi.org/10.1371/journal.pgen.1001176.

Lappalainen, P., Drubin, D.G., 1997. Cofilin promotes rapid actin filament turnover in vivo. Nature 388, 78–82. http://dx.doi.org/10.1038/40418.

Lee, Y.J., Mazzatti, D.J., Yun, Z., Keng, P.C., 2005. Inhibition of invasiveness of human lung cancer cell line H1299 by over-expression of cofilin. Cell Biol. Int. 29, 877–883. http://dx.doi.org/10.1016/j.cellbi.2005.07.005.

Lee, S.I., Kim, D.S., Lee, H.J., Cha, H.J., Kim, E.C., 2013. The role of thymosin beta 4 on odontogenic differentiation in human dental pulp cells. PLoS One 8, e61960. http://dx.doi.org/10.1371/journal.pone.0061960.

Liu, Y., Ross, J.F., Bodine, P.V., Billiard, J., 2007. Homodimerization of Ror2 tyrosine kinase receptor induces 14-3-3(beta) phosphorylation and promotes osteoblast differentiation and bone formation. Mol. Endocrinol. 21, 3050–3061. http://dx.doi.org/10.1210/me.2007-0323.

Lodish, H., Berk, A., Z, L.S., Matsudaira, P., Baltimore, D., D, J., 2000. Molecular Cell Biology. W. H. Freeman and Company, New York.

Lomri, A., Marie, P.J., Escurat, M., Portier, M.M., 1987. Cytoskeletal protein synthesis and organization in cultured mouse osteoblastic cells. Effects of cell density. FEBS Lett. 222, 311–316.

Loty, S., Forest, N., Boulekbache, H., Sautier, J.M., 1995. Cytochalasin D induces changes in cell shape and promotes in vitro chondrogenesis: a morphological study. Biol. Cell. 83, 149–161.

Maekawa, M., Ishizaki, T., Boku, S., Watanabe, N., Fujita, A., Iwamatsu, A., Obinata, T., Ohashi, K., Mizuno, K., Narumiya, S., 1999. Signaling from Rho to the actin cytoskeleton through protein kinases ROCK and LIM-kinase. Science 285, 895–898.

Mathews, S., Bhonde, R., Gupta, P.K., Totey, S., 2012. Extracellular matrix protein mediated regulation of the osteoblast differentiation of bone marrow derived human mesenchymal stem cells. Differentiation 84, 185–192. http://dx.doi.org/10.1016/j.diff.2012.05.001.

McBeath, R., Pirone, D.M., Nelson, C.M., Bhadriraju, K., Chen, C.S., 2004. Cell shape, cytoskeletal tension, and RhoA regulate stem cell lineage commitment. Dev. Cell 6, 483–495.

Niwa, R., Nagata-Ohashi, K., Takeichi, M., Mizuno, K., Uemura, T., 2002. Control of actin reorganization by Slingshot, a family of phosphatases that dephosphorylate ADF/cofilin. Cell 108, 233–246.

Nurminsky, D., Magee, C., Faverman, L., Nurminskaya, M., 2007. Regulation of chondrocyte differentiation by actin-severing protein adseverin. Dev. Biol. 302, 427–437. http://dx.doi.org/10.1016/j.ydbio.2006.09.052.

Ono, S., 2007. Mechanism of depolymerization and severing of actin filaments and its significance in cytoskeletal dynamics. Int. Rev. Cytol. 258, 1–82. http://dx.doi.org/10.1016/S0074-7696(07)58001-0.

Pho, M., Lee, W., Watt, D.R., Laschinger, C., Simmons, C.A., McCulloch, C.A., 2008. Cofilin is a marker of myofibroblast differentiation in cells from porcine aortic cardiac valves.

Am. J. Physiol. Heart Circ. Physiol. 294, H1767–H1778. http://dx.doi.org/10.1152/ajpheart.01305.2007.
Pope, B.J., Zierler-Gould, K.M., Kuhne, R., Weeds, A.G., Ball, L.J., 2004. Solution structure of human cofilin: actin binding, pH sensitivity, and relationship to actin-depolymerizing factor. J. Biol. Chem. 279, 4840–4848. http://dx.doi.org/10.1074/jbc.M310148200.
Prowse, P.D., Elliott, C.G., Hutter, J., Hamilton, D.W., 2013. Inhibition of Rac and ROCK signalling influence osteoblast adhesion, differentiation and mineralization on titanium topographies. PLoS One 8, e58898. http://dx.doi.org/10.1371/journal.pone.0058898.
Rodriguez, J.P., Gonzalez, M., Rios, S., Cambiazo, V., 2004. Cytoskeletal organization of human mesenchymal stem cells (MSC) changes during their osteogenic differentiation. J. Cell. Biochem. 93, 721–731. http://dx.doi.org/10.1002/jcb.20234.
Sakai, D., Kii, I., Nakagawa, K., Matsumoto, H.N., Takahashi, M., Yoshida, S., Hosoya, T., Takakuda, K., Kudo, A., 2011. Remodeling of actin cytoskeleton in mouse periosteal cells under mechanical loading induces periosteal cell proliferation during bone formation. PLoS One 6, e24847. http://dx.doi.org/10.1371/journal.pone.0024847.
Shuang, F., Sun, Y., Yang, H.H., Shao, Y.C., Li, H., Hu, W., Zhong, J., Zou, H.X., 2013. Destrin deletion enhances the bone loss in hindlimb suspended mice. Eur. J. Appl. Physiol. 113, 403–410. http://dx.doi.org/10.1007/s00421-012-2451-4.
Simonsen, J.L., Rosada, C., Serakinci, N., Justesen, J., Stenderup, K., Rattan, S.I., Jensen, T.G., Kassem, M., 2002. Telomerase expression extends the proliferative life-span and maintains the osteogenic potential of human bone marrow stromal cells. Nat. Biotechnol. 20, 592–596. http://dx.doi.org/10.1038/nbt0602-592.
Someya, H., Fujiwara, H., Nagata, K., Wada, H., Hasegawa, K., Mikami, Y., Jinno, A., Sakai, H., Koyano, K., Kiyoshima, T., 2015. Thymosin beta 4 is associated with RUNX2 expression through the Smad and Akt signaling pathways in mouse dental epithelial cells. Int. J. Mol. Med. 35, 1169–1178. http://dx.doi.org/10.3892/ijmm.2015.2118.
Sonowal, H., Kumar, A., Bhattacharyya, J., Gogoi, P.K., Jaganathan, B.G., 2013. Inhibition of actin polymerization decreases osteogeneic differentiation of mesenchymal stem cells through p38 MAPK pathway. J. Biomed. Sci. 20, 71. http://dx.doi.org/10.1186/1423-0127-20-71.
Stenderup, K., Rosada, C., Justesen, J., Al-Soubky, T., Dagnaes-Hansen, F., Kassem, M., 2004. Aged human bone marrow stromal cells maintaining bone forming capacity in vivo evaluated using an improved method of visualization. Biogerontology 5, 107–118. http://dx.doi.org/10.1023/B:BGEN.0000025074.88476.e2.
Toshima, J., Toshima, J.Y., Amano, T., Yang, N., Narumiya, S., Mizuno, K., 2001. Cofilin phosphorylation by protein kinase testicular protein kinase 1 and its role in integrin-mediated actin reorganization and focal adhesion formation. Mol. Biol. Cell 12, 1131–1145.
Treiser, M.D., Yang, E.H., Gordonov, S., Cohen, D.M., Androulakis, I.P., Kohn, J., Chen, C.S., Moghe, P.V., 2010. Cytoskeleton-based forecasting of stem cell lineage fates. Proc. Natl. Acad. Sci. U. S. A. 107, 610–615. http://dx.doi.org/10.1073/pnas.0909597107.
Tsai, C.H., Chiu, S.J., Liu, C.C., Sheu, T.J., Hsieh, C.H., Keng, P.C., Lee, Y.J., 2009. Regulated expression of cofilin and the consequent regulation of p27(kip1) are essential for G(1) phase progression. Cell Cycle 8, 2365–2374.
Van Troys, M., Huyck, L., Leyman, S., Dhaese, S., Vandekerkhove, J., Ampe, C., 2008. Ins and outs of ADF/cofilin activity and regulation. Eur. J. Cell Biol. 87, 649–667. http://dx.doi.org/10.1016/j.ejcb.2008.04.001.
Vartiainen, M.K., Mustonen, T., Mattila, P.K., Ojala, P.J., Thesleff, I., Partanen, J., Lappalainen, P., 2002. The three mouse actin-depolymerizing factor/cofilins evolved to fulfill cell-type-specific requirements for actin dynamics. Mol. Biol. Cell 13, 183–194. http://dx.doi.org/10.1091/mbc.01-07-0331.
Wang, D.B., Xu, Y.L., Chen, P., Chen, Y.H., Li, Y., 2013. Silencing Cofilin-1 blocks PDGF-induced proliferation in eutopic endometrium of endometriosis patients. Cell Biol. Int. 37, 799–804. http://dx.doi.org/10.1002/cbin.10093.
Warn, R.M., Magrath, R., 1983. F-actin distribution during the cellularization of the Drosophila embryo visualized with FL-phalloidin. Exp. Cell Res. 143, 103–114.
Won, K.J., Park, S.H., Park, T., Lee, C.K., Lee, H.M., Choi, W.S., Kim, S.J., Park, P.J., Jang, H.K., Kim, S.H., Kim, B., 2008. Cofilin phosphorylation mediates proliferation in response to platelet-derived growth factor-BB in rat aortic smooth muscle cells. J. Pharmacol. Sci. 108, 372–379.
Woods, A., Wang, G., Beier, F., 2005. RhoA/ROCK signaling regulates Sox9 expression and actin organization during chondrogenesis. J. Biol. Chem. 280, 11626–11634. http://dx.doi.org/10.1074/jbc.M409158200.
Woods, A., Wang, G., Beier, F., 2007. Regulation of chondrocyte differentiation by the actin cytoskeleton and adhesive interactions. J. Cell. Physiol. 213, 1–8. http://dx.doi.org/10.1002/jcp.21110.
Xu, J., Wang, W., Ludeman, M., Cheng, K., Hayami, T., Lotz, J.C., Kapila, S., 2008. Chondrogenic differentiation of human mesenchymal stem cells in three-dimensional alginate gels. Tissue Eng. A 14, 667–680. http://dx.doi.org/10.1089/tea.2007.0272.
Yamashita, M., Otsuka, F., Mukai, T., Otani, H., Inagaki, K., Miyoshi, T., Goto, J., Yamamura, M., Makino, H., 2008. Simvastatin antagonizes tumor necrosis factor-alpha inhibition of bone morphogenetic proteins-2-induced osteoblast differentiation by regulating Smad signaling and Ras/Rho-mitogen-activated protein kinase pathway. J. Endocrinol. 196, 601–613. http://dx.doi.org/10.1677/JOE-07-0532.
Yang, N., Higuchi, O., Ohashi, K., Nagata, K., Wada, A., Kangawa, K., Nishida, E., Mizuno, K., 1998. Cofilin phosphorylation by LIM-kinase 1 and its role in Rac-mediated actin reorganization. Nature 393, 809–812. http://dx.doi.org/10.1038/31735.
Yeoh, S., Pope, B., Mannherz, H.G., Weeds, A., 2002. Determining the differences in actin binding by human ADF and cofilin. J. Mol. Biol. 315, 911–925. http://dx.doi.org/10.1006/jmbi.2001.5280.
Yourek, G., Hussain, M.A., Mao, J.J., 2007. Cytoskeletal changes of mesenchymal stem cells during differentiation. ASAIO J. 53, 219–228. http://dx.doi.org/10.1097/MAT.0b013e31802deb2d.
Zigmond, S.H., 1996. Signal transduction and actin filament organization. Curr. Opin. Cell Biol. 8, 66–73.